Improving GCM Aerosol Climatology using Satellite and Ground-Based Measurements

L. Liu
Department of Applied Physics and Applied Mathematics
Columbia University
New York, New York

A.A. Lacis, B.E. Carlson, M.I. Mishchenko, and B. Cairns
NASA Goddard Institute for Space Studies
New York, New York

Abstract

A physically based aerosol climatology is essential to address the questions of global climate changes. We use available satellite and ground-based measurements, i.e., moderate-resolution imaging spectroradiometer (MODIS), multiangle imaging spectroradiometer (MISR), Polarization and Directionality of the earth's Reflectance (POLDER), advanced very high resolution radiometer (AVHRR), and Aerosol Robotic Network (AERONET) data, to characterize the geographic distribution and seasonal variability of aerosol optical depth and size. The Ångström exponent is used as a measure of aerosol size. Although large discrepancies exist between different datasets, particularly for the Ångström exponent, the measurements point to a need for reducing the aerosol effective radii specified in the global climate model (GCM) from the nearly 1.0 micron average value to about 0.2 or 0.3 microns, as suggested by the observed Ångström exponent. Incorporating this change in aerosol effective radius also improves the agreement for the aerosol optical depth between satellite measurements and the Goddard Institute for Space Studies (GISS) GCM aerosol climatology. As a consequence, the radiative forcing due to aerosol under clear-sky conditions is increased by about 30%.

Motivation

The impact of aerosols on the global climate system through their direct, semi-direct, and indirect radiative forcing is one of the major uncertainties in present climate modeling studies (Charlson et al. 1992; Hansen et al. 1995, 1997a,b, 2000). Unlike well-mixed greenhouse gases, the radiative forcing due to aerosols has been difficult to define accurately, partly because of the high spatial inhomogeneity and significant temporal variability of aerosols. A physically based GCM aerosol climatology is essential to address the questions of global climate changes. The SI2000 version of the GISS GCM is described in detail by Hansen et al. (2002). The description of the treatment of tropospheric aerosols in the GCM is given in Section 2.6 of the paper. Despite the various improvements documented in that publication, the SI2000 aerosol is still a crude representation of real world aerosols. For example, the effective radii are rather arbitrarily specified to convert mass loadings from transport model simulations

into optical depths that are in reasonable accord with the total atmospheric aerosol load; sulfate and sea salt sizes are specified as globally constant and include a climatological, instead of than explicit dependence on relative humidity; similarly, black carbon from industrial and biomass burning is fixed in size; also, the SI2000 model does not include nitrate aerosols which are becoming increasingly more important. The principal objective of this paper is to use the available satellite and ground-based measurements, i.e., MODIS, MISR, POLDER, AVHRR, and AERONET data, to characterize and validate the geographic distribution and seasonal variability of our GCM aerosol climatology.

Aerosol optical depth (AOD, also widely denoted as τ) is a common variable to connect the model and measurements. AOD is in general a standard product of satellite retrievals as well as a routinely measured quantity in field campaigns. Given the model-simulated atmospheric distributions and composition of aerosols, the aerosol optical depth can be calculated provided that the complex refractive indices, size distributions, and hygroscopic properties of aerosols are known. Aerosol mass loading per unit area M and optical depth are related by (Lacis and Mischenko 1994),

$$\tau = \frac{3Q_{ext}M}{4\rho r_{eff}} \qquad (1)$$

Where ρ the specific density of the aerosol, Q_{ext} is the extinction efficiency factor, r_{eff} is the effective radius (cross section weighted radius over the size distribution [Hansen and Travis 1974]). Ångström exponent (A, also widely known as α), a measure of the average particle size, is the second most important variable of satellite products which is typically computed using

$$A = -\ln(\tau_{\lambda_1}/\tau_{\lambda_2})/\ln(\lambda_1/\lambda_2). \qquad (2)$$

Ångström exponent is inversely proportional to particle size, i.e., higher A values usually are associated with smaller aerosols. The GCM radiation model does not explicitly use the Ångström exponent, but this appears to be a better indicator of aerosol size than the effective radius when the aerosol has a complicated size distribution (i.e., bi-mode or multi-mode size distribution).

To our knowledge, previous model validation efforts (i.e., Penner et al. 2002; Chin et al. 2002) all focus on comparing model generated aerosol optical depths with those derived by satellite and field sun-photometer measurements. A more accurate estimate of the effective radius is essential (as can be seen in Eq. 1) to achieve the required accuracy in AOD to quantify aerosol radiative forcing. So in this study, we not only compare the GCM aerosol optical depth but also the Ångström exponent climatology under clear sky conditions with satellite products. As we all know remote sensing of aerosols is possible only when there is no presence of clouds.

Results

Figures 1 and 2 show overall monthly mean optical depths at a wavelength $\lambda = 0.55$ μm and Ångström exponent in July complied from the whole data record for different aerosol datasets. Top right hand side numbers represent the corresponding area weighted global means. To directly compare with the model results, we have degraded the satellite retrievals into the 4° x 5° GCM grid resolution using equal

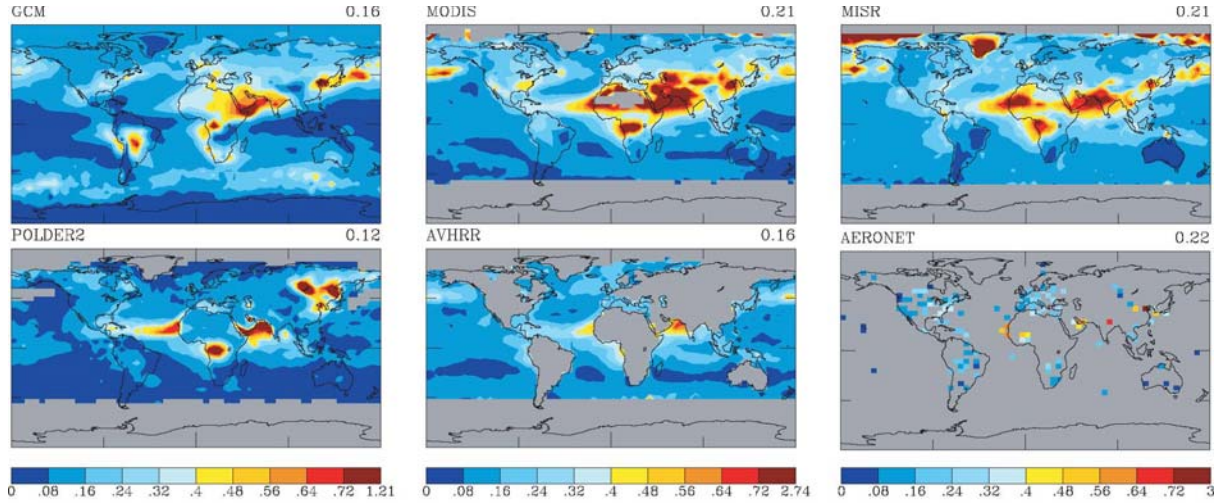

Figure 1. Global distributions of aerosol overall monthly averaged optical depths at 0.55 μm in July compiled from different datasets. The numbers on the top right corners represent global area weighted means.

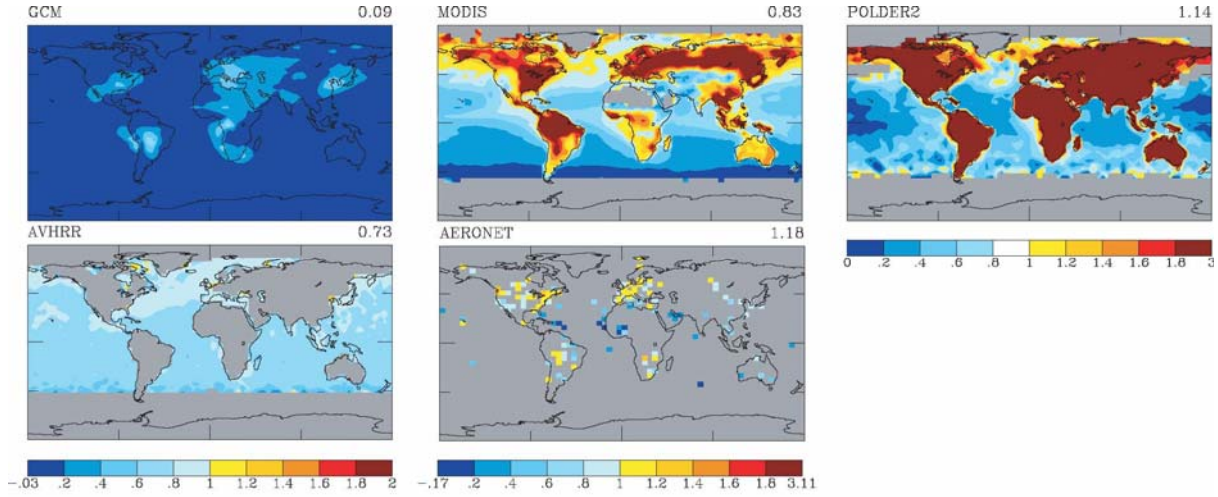

Figure 2. As in Figure 1, but for Ångström exponents.

weights. If there is more than one AERONET site in a GCM grid box, the data are combined with equal weights. It is clear that the general patterns of the AOD global distributions are rather similar to each other. The model produces the prominent features of geographical variations of AODs as observed by the satellites, such as dust plumes over northern Africa and the Persian Gulf region, smoke in Southern Africa, etc. The aerosol loadings are higher over land and near coasts. The values decline with distance away from the continental sources, consistent with the mechanisms of aerosol transport by large-scale wind system and deposition. Overall, the air is much cleaner over open oceans, i.e., Central Pacific Ocean. GCM produces an aerosol plume possibly related with biomass burning in South America. This phenomenon however has not been observed by any of the satellite and ground measurements. High aerosol concentrations are reported by MISR over the northern polar region. This may be attributed to the difficulties detecting clouds over snow and ice surfaces. The AVHRR retrievals tend to produce

smaller values in areas with high aerosol loads. It is no surprise that substantial differences exist for Ångström exponent between different datasets. The accuracy of A is lower than that of aerosol optical depth since the Ångström exponent is derived from the derivatives of the AODs between two wavelengths (Eq. 2), and is inversely proportional to aerosol optical depth. A small error in the retrieved AODs would transform to a much larger offset in the calculated Ångström exponent. The A values of the GCM aerosol climatology are essentially close to 0 without much spatial variation. The underlying reason is that in the model the averaged particle size is preset to about 1 μm (therefore small A values) to convert the chemistry transport model simulated atmospheric aerosol burdens to optical depth. The transition from smaller anthropogenically influenced continental particulates to generally larger oceanic aerosols can be easily discerned from the satellite derived Ångström exponents. Such trend of variation is less clear for AVHRR retrievals (Figure 2), which tends to be more or less global uniform. The POLDER retrieved Ångström exponents are much higher over land because the remote sensing technique based on the polarization signature of scattered solar radiances is only sensitive to particles that are within the accumulation mode. The combined observations of aerosol burden and size as characterized by A suggest that in general the aerosols are large sized and lower in concentration over the ocean. While small particles produced by anthropogenic sources, like smoke and urban/industrial aerosols, are mostly found over civilized land and in coastal zones.

The relationship between Ångström exponent versus effective radius for different size distributions are depicted in Figure 3. The aerosols considered are absorptive with refractive index of 1.5 + 0.003i. Obviously, for the same effective radius r_{eff} and effective variance v_{eff} (Hansen and Travis 1974), the computed A is not particularly sensitive to the variations of aerosol size distribution provided that it is mono-mode, and not shown in the figure the selections of the pair of the wavelengths. An Ångström exponent close to 1 corresponds to accumulation mode aerosols with effective radius of about 0.2 – 0.3 μm, while zero A values are associated with coarse particles with r_{eff} about 1 μm or larger. The steep slope between A and r_{eff} for the effective radii range from about 0.06 to 0.4 μm indicates the need to increase the retrieval accuracy of A to get the aerosol size right.

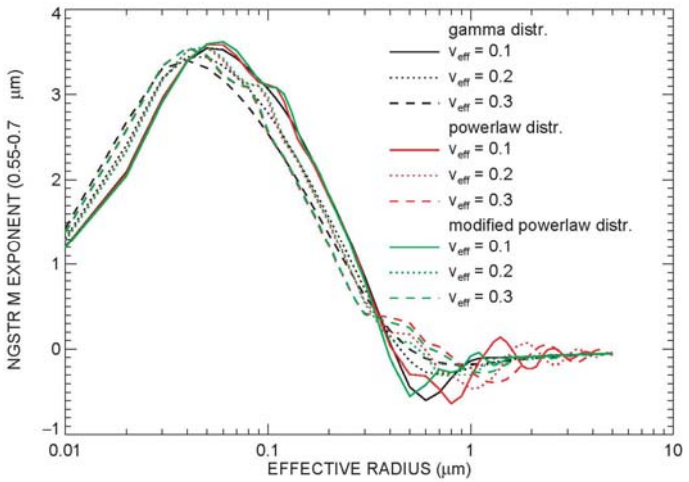

Figure 3. Ångström exponent computed between 0.55 and 0.7 μm versus effective radius for different size distributions. The refractive index is 1.5 + 0.003 i.

Figure 4 has demonstrated the differences in monthly averaged aerosol optical depths over land and ocean, and the land and ocean areas constrained between 45°S–45°N. The averages are computed from the whole data record for each dataset. Please note since different aerosol retrieval algorithms are utilized over land and ocean for some of the sensors, i.e., MODIS, POLDER and MISR, and the properties of continental and maritime aerosols are remarkably different, we compare the retrieved aerosol parameters over land and ocean with GCM aerosol climatology individually. On average, AOD_{MODIS} (red curves) are systematically higher than AOD_{MISR} (orange curves) by about 0.075 over land and lower by about 0.043 over ocean. Abdou et al. (2005) report that MODIS values bias high over land and MISR values bias high over ocean by comparing MISR and MODIS optical depths with each other and with AERONET measurements. This is consistent with what we have found in this study. Despite lower in magnitude, the reprocessed POLDER2 AOD data (represented by thick blue curves) using the second generation algorithms resemble MODIS and MISR well with the highest value occurring during summer and lowest one in winter season. We expect reprocessing POLDER 1 data (shown by thin blue curves) using the new retrieval techniques would improve the consistency with other satellite products. In contrast to MODIS, MISR, and POLDER2 data, the annual variability pattern of the globally averaged AODs for AVHRR retrievals reaches maxima around January – February and minima in June – July (also reported by Geogdzhayev et al. 2002). The GCM aerosol optical depths agree with satellite measurements rather well considering the uncertainties related with satellite retrievals. In general its AOD values (represented by black curves) are lower than other datasets except POLDER. Although the maximum value of GCM modeled AODs occurred at the same summer season as MODIS, MISR and POLDER2, the seasonality differs somewhat. Since most AERONET data depicted by green curves on the left panels of Figure 4 are collected over land with few coastal and island sites, we take into consideration all the measurements available without distinguishing land and ocean sites and compare them with other aerosol land data. Of course one can always question the representativeness of the AERONET-measured aerosols to the global tropospheric aerosols. Excluding the data beyond the 45°S – 45°N belt as satellite retrievals become less reliable at high latitudes due to potential cloud contaminations, high surface albedo and zenith angle improve the agreement between different datasets over both land and ocean.

Similar to Figure 4, Figure 5 presents the differences in multi-year monthly averaged aerosol Ångström exponents over land and ocean, and the land and ocean areas constrained between 45°S–45°N for different datasets. The range of A varies from about 0.05 of GCM to about 0.75 of AVHRR over the ocean, and from about 0.15 of GCM to about 2.5 of POLDER over the land. The A_{land} are significantly higher than A_{ocean}, consistent with our knowledge that oceanic aerosols are large sized while anthropogenic aerosols originated from fossil fuel and biomass burning are usually in the accumulation mode of aerosols. The seasonality of global Ångström exponent over the land for MODIS and AERONET are very similar largely due to the tuning effects.

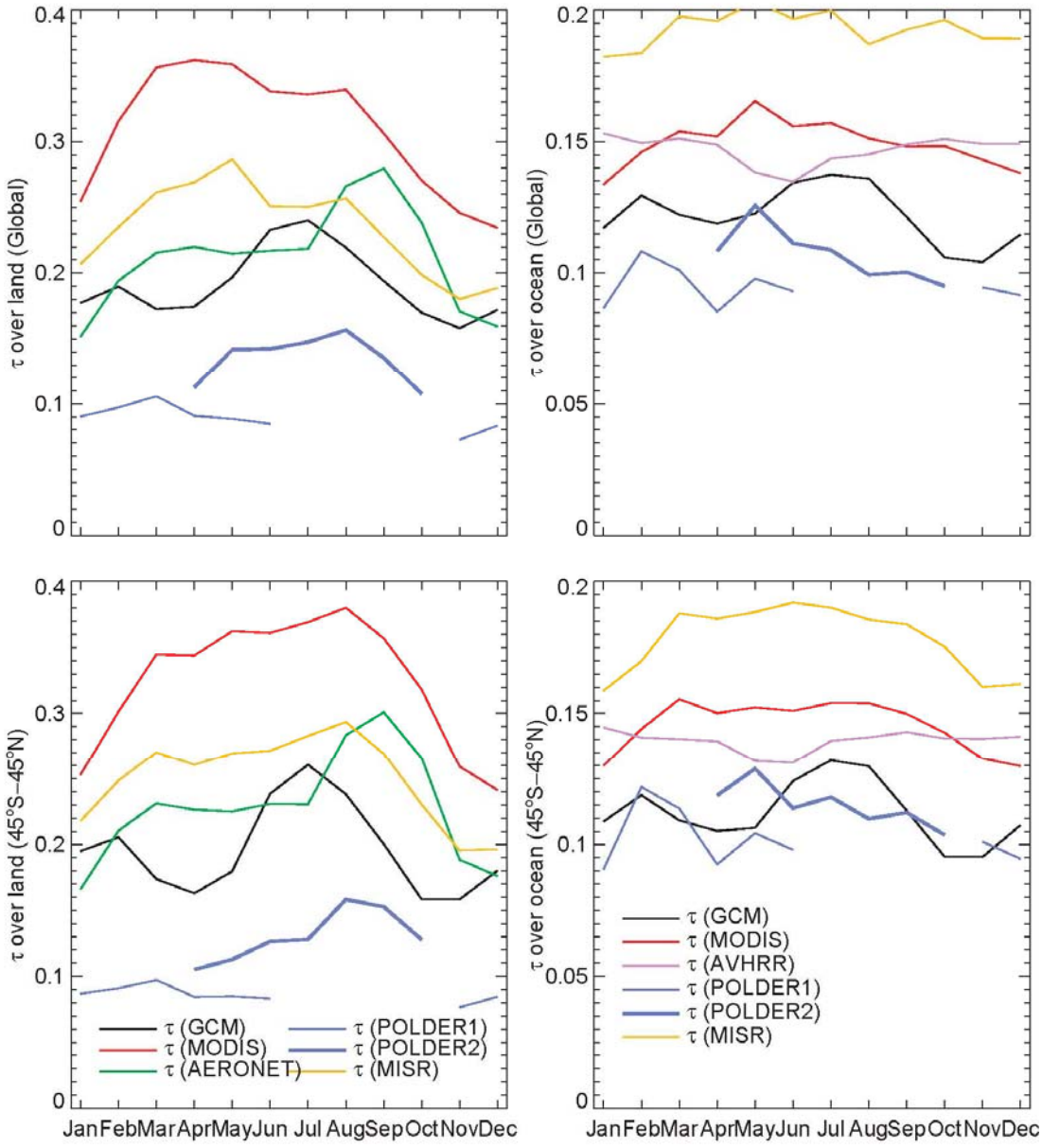

Figure 4. Comparisons of GISS GCM and satellite retrieved global area weighted monthly means of aerosol optical depths at 0.55 μm. The monthly averages are calculated from the entire length of the data available.

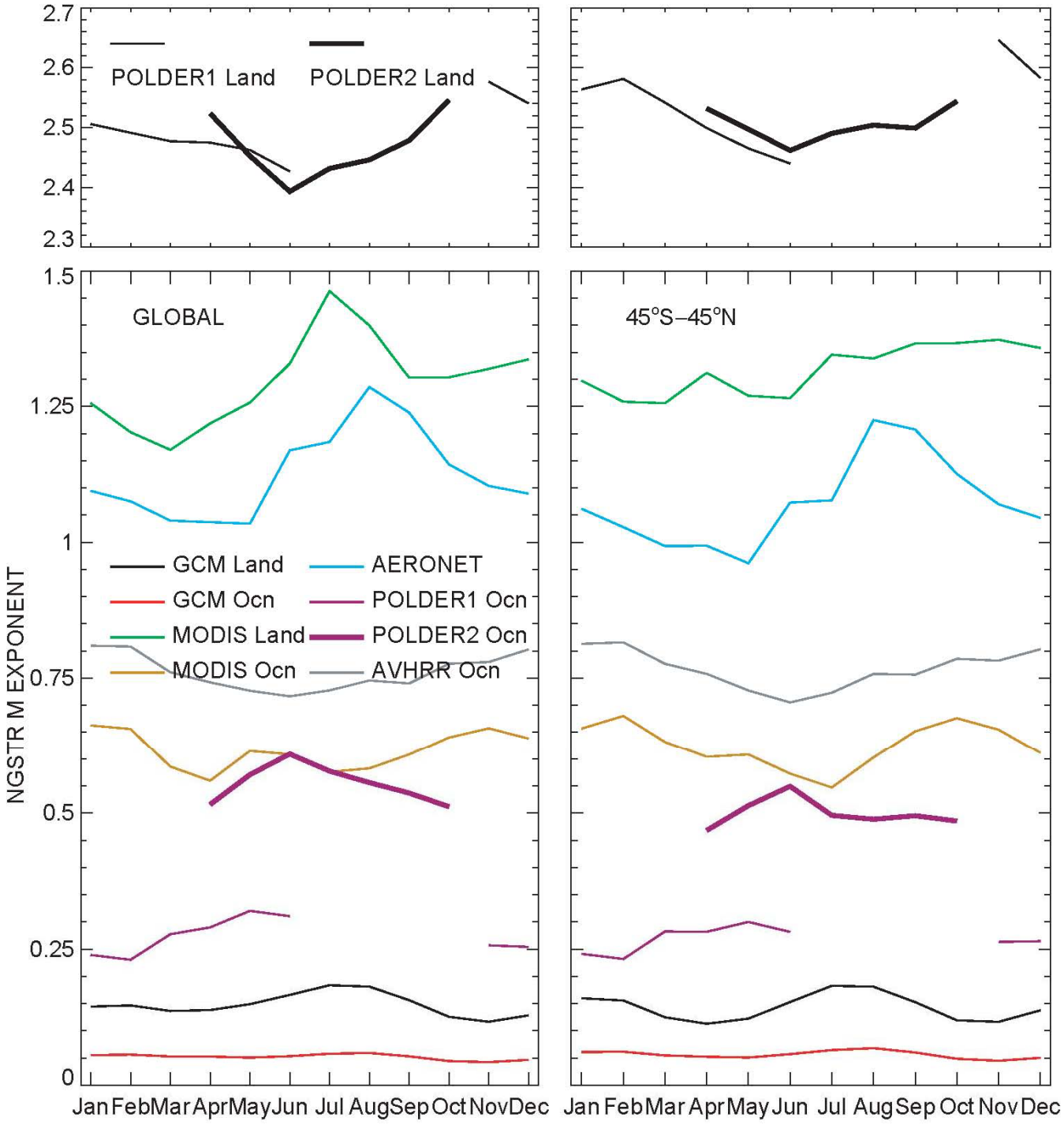

Figure 5. As in Figure 4, but for Ångström exponents.

The frequency of occurrence distributions for overall monthly averaged aerosol optical depth and Ångström exponent in July are shown in Figures 6 and 7. The data selected are limited to between 45°S – 45°N because satellite products become less reliable at higher latitude. The frequency

histograms of AOD demonstrate that the majority of the values are less than 0.15 over oceans with the most frequently occurring values between 0.05 to 0.125 for GCM, 0.075 to 0.125 for MODIS, 0.1 to 0.15 for MISR, 0.025 to 0.1 for POLDER2, and 0.075 to 0.125 for AVHRR. The AOD probability distributions over the land are much more broader for all the datasets except POLDER2 whose AOD values are mostly smaller than 0.2. Figure 7 demonstrates that there is 75% of the chance that AGCM over oceans fall into the 0 – 0.1 bracket and about 81% AGCM values over the land are between 0 and 0.3, while the frequency histograms for MOIDS and AERONET are broader with A between about 0 to 1 over the oceans and between about 0 to more than 2 over the land. This once again may imply that the averaged effective radius may be specified too high in the GCM.

Figure 8 shows the time series of the model simulated and the satellite retrieved global and hemispherical monthly means of the aerosol optical depth and Ångström exponent over land and ocean starting from 1996 when POLDER 1 was launched to the space. Since the GCM aerosol climatology in the industrial era are computed for 1990, we arbitrarily place the curves starting from January 1996 in the figure and let the annual cycle repeat itself up to four years for comparison purposes. One can see a generally reasonable agreement between the GCM AOD climatology and the satellite measurements. The most common and distinguished feature is that the average aerosol load is much higher in the northern hemisphere (NH) than southern hemisphere (SH). The global average shows a smaller annual variability compared with the seasonal amplitude of the NH and SH individually. The AOD time series show clear seasonal patterns in NH and SH for MODIS (Terra and Aqua), and MISR. The NH peaks in late spring and early summer, while the SH is highest in October – December (late spring and early summer in SH). The high spike of AOD_{Aqua} reaching up almost to 0.4 in May 2003 over the ocean is caused by some unphysical results over Artic region (AOD = 5, the highest allowable value in the MODIS retrieval algorithms). The comparison of the Ångström exponent records reveals large fluctuations. Similar to AOD, this parameter is also larger in NH than SH and constantly higher in value over the land than oceans. Very little seasonal variations in A exist for GCM. Interestingly the MODIS derived A values are always in phase with their AOD retrievals reaching the maxima and minima at the same time. The abrupt change in the AVHRR-derived A values at the end of the record is associated with the orbital shift and general deterioration of the quality of the AVHRR radiance data, and the large shift in the MODIS-retrieved A values in June 2001 is due to the switch of electronics from A-side to B-side. Despite using the same sensor, appreciable differences exist between MODIS Terra and Aqua with A_{Aqua} significantly larger than A_{Terra}, particularly during year 2003. The gap seems to be closed up quite significantly in 2004. Since Terra's orbit around the Earth is timed so that it passes from north to south across the equator at 10:30 a.m. in the morning, while Aqua passes south to north over the equator at 1:30 p.m. in the afternoon. Our first guess is that it might be caused by aerosol diurnal variability, which unfortunately cannot induce such big differences. The only possible reasons might be related with calibration, different retrieval algorithms and cloud screening techniques.

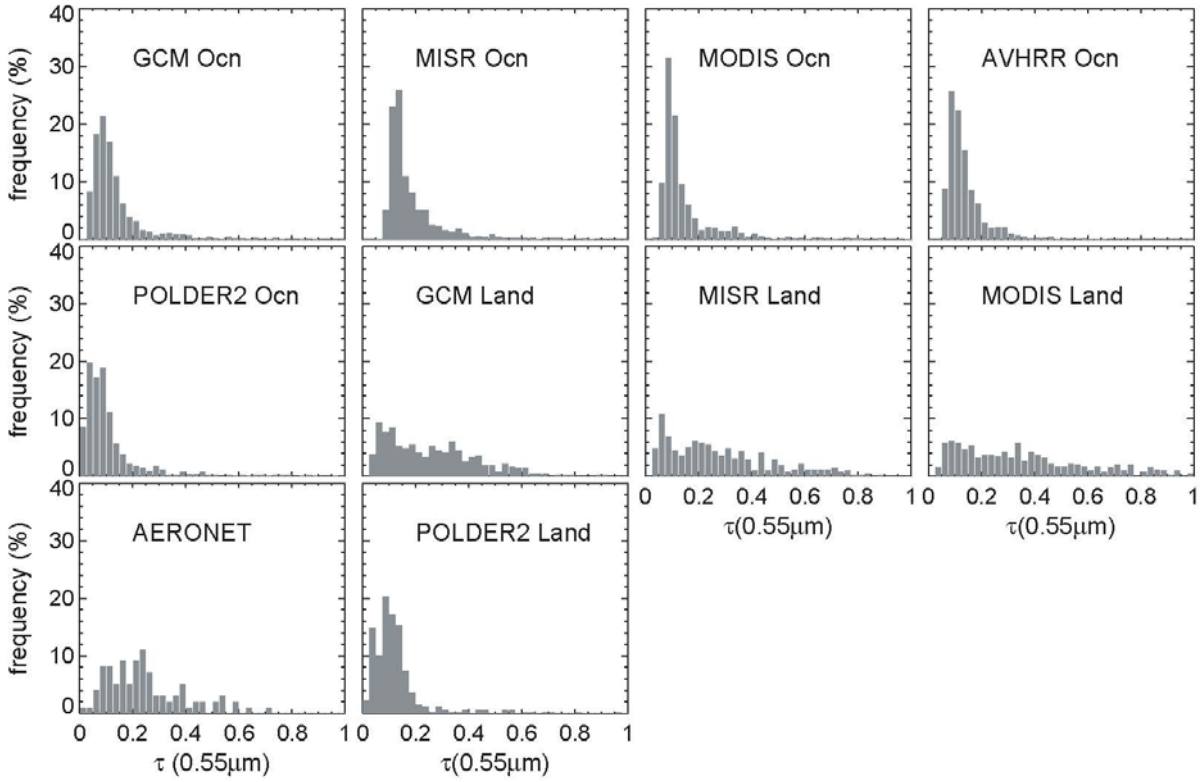

Figure 6. Frequency distributions of aerosol optical depth monthly averages at 0.55 μm in July composed from multi-year data record for different datasets. The data are constrained between 45°S – 45°N.

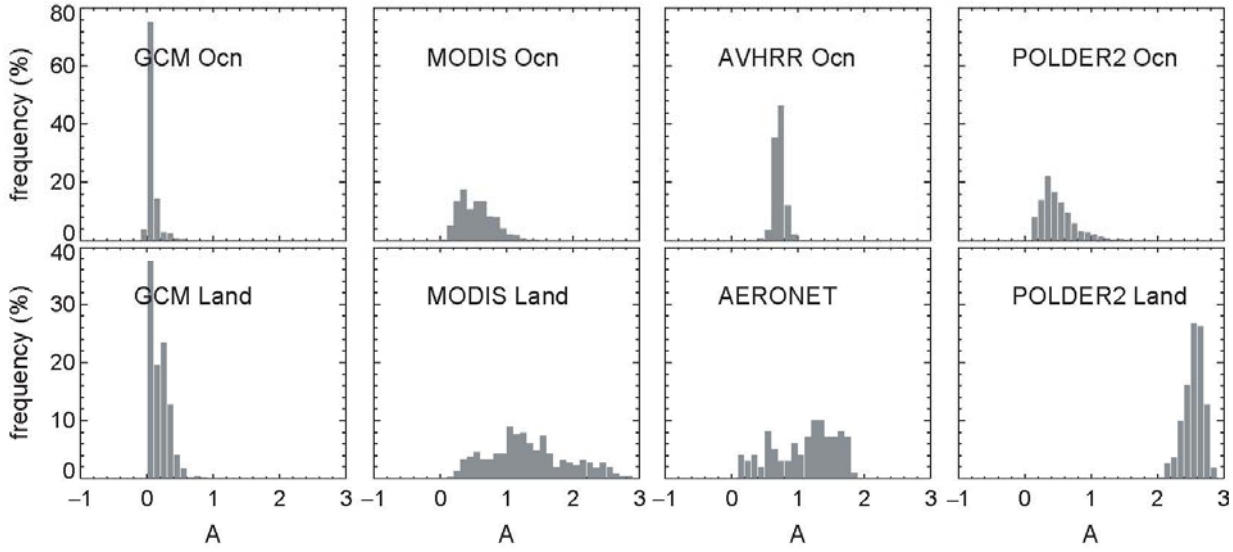

Figure 7. Similar to Figure 6, but for frequency of occurrences of monthly mean Ångström exponents in July. The data considered are confined between 45°S – 45°N.

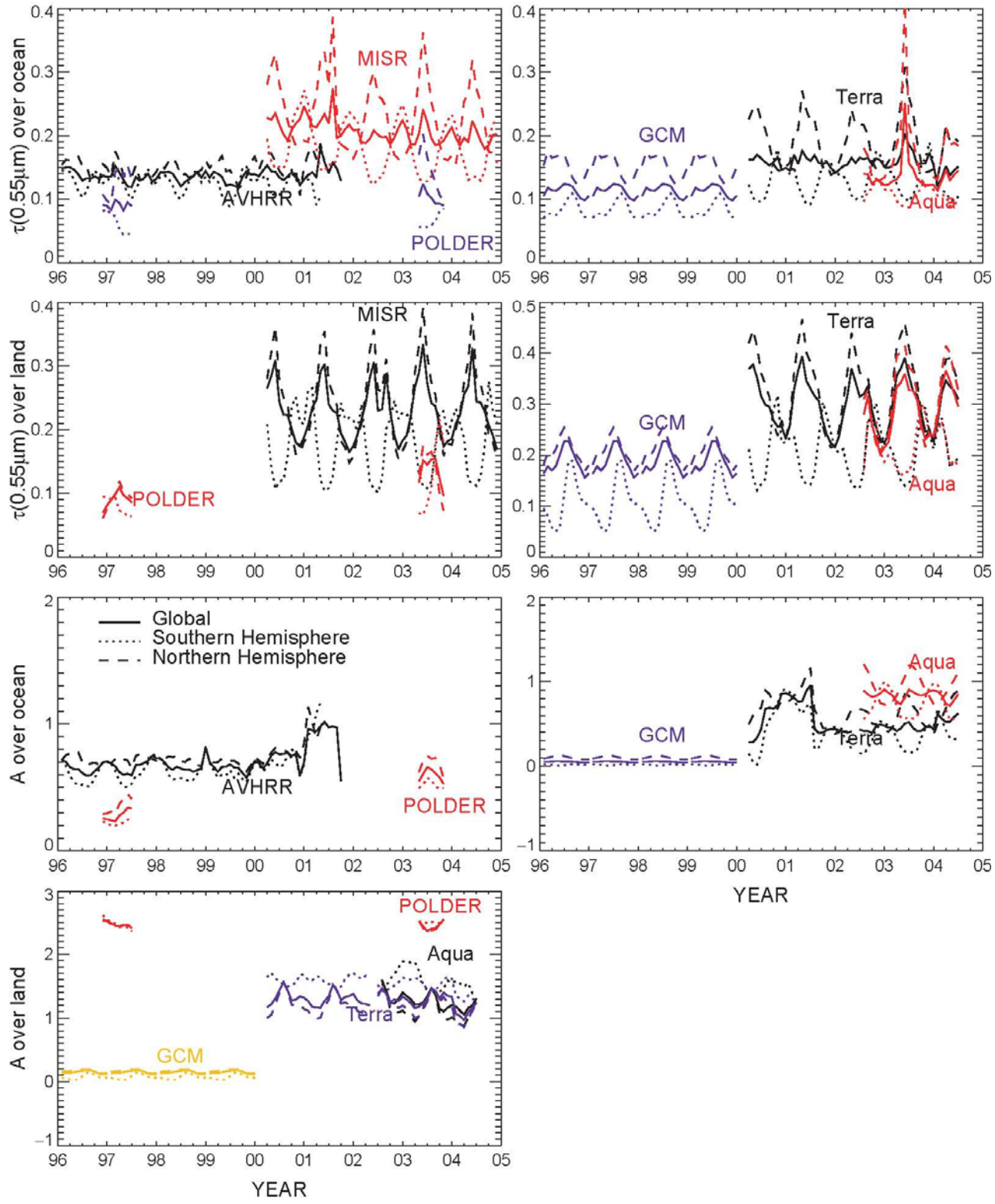

Figure 8. Time series of the satellite retrieved global and hemispherical monthly mean aerosol optical depths and Ångström exponents and GCM aerosol climatology.

Figure 9 is the scattering plot of all the available AERONET measured monthly (January – December) mean values of aerosol optical depths and Ångström exponents versus the corresponding model results. The AERONET averages are calculated from the entire length of the sun-photometer measurements at each site and then averaged if available into each GCM grid box. It is clear that the model generated A are significantly under-estimated compared with that of the AERONET data. The global averaged A over oceans compiled from the historical ship measurements (table 1 of Liu et al. 2004) is 0.78, which is another manifestation of too low A values. Overall AODGCM and AODAERONET reasonably well with a correlation coefficient greater than 0.5.

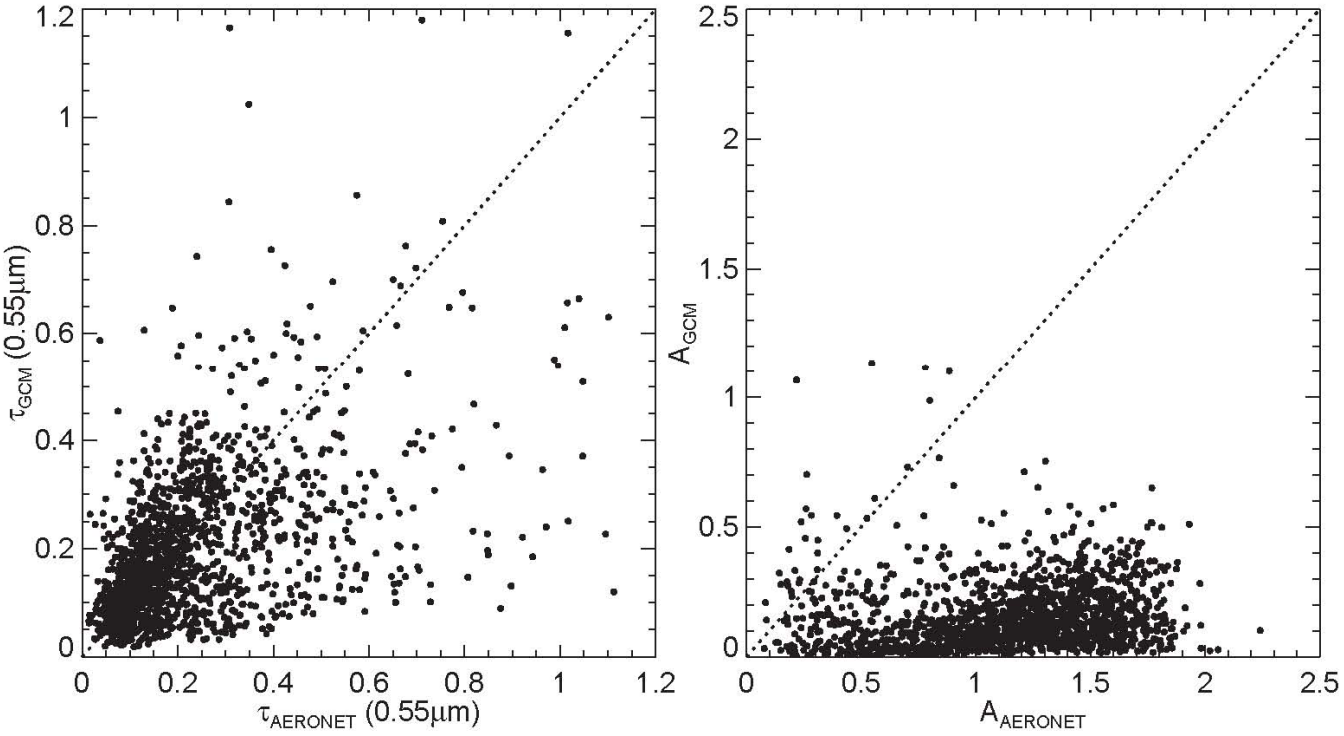

Figure 9. GCM aerosol climatology versus AERONET observed overall monthly mean values of AOD and A. The AERONET data were averaged into 4° by 5° GCM grid box resolution using equal weight provided the data are available. The dotted line depicts the 1:1 relationship.

Summary

Large uncertainties are involved in deriving the AODs from both the model and satellite measurements. The accuracy for each of the satellite datasets has been estimated by various validation studies, which are outlined above. Here we will discuss a few uncertainties relevant to model optical depth outputs. Numerous factors such as column mass loading M, extinction efficiency factor Q_{ext}, effective radius r_{eff}, and aerosol specific density ρ (Eq. 1) constrain the accuracy of modeled AOD. The mass loading for each aerosol species is determined by the sources, transport and removal processes, and the hygroscopic properties of the aerosols. Errors in aerosol emission and uncertainties in the consequent transport and deposition processes have a direct effect on model calculated optical depth. The extinction efficiency factor for each type of aerosols is mainly determined by the size distribution, refractive index, particle

shape, and hygroscopic growth rate of the aerosols. At present these properties are highly parameterized based on quite limited measurements. The effective radius is mainly decided by highly variable aerosol size distribution. And there is a wide range of uncertainties in specific density for certain types of aerosols, i.e., from less than 1 to more than 2 g/cm^3 for black carbon (Fuller et al. 1999). All of these would result in final uncertainties in aerosol optical depths. Our validation study shows that decreasing particle effective radius is a right direction to improve our GCM aerosol climatology for the reason of reducing particle effective radius not only would result in higher Ångström exponents which are more consistent with satellite and ground sun-photometer measurements, but also increase modeled aerosol optical depths which are biased a little low.

In summary, substantial discrepancies exist between different datasets, particularly for Ångström exponent. The overall globally averaged aerosol optical depth monthly means range from about 0.08 to 0.36 over land and from about 0.08 to 0.2 over ocean, and the A values vary from about 0 to more than 2, representing coarse and fine aerosols respectively. Generally speaking, in terms of aerosol seasonality, MISR and MODIS data agree with each other better than other satellite retrievals and GCM aerosol outputs with the maxima of AODs occurring around May-June and the minima in December-January over ocean. This is not a surprise since the sensors are more advanced and much better calibrated than other old generation instruments. There are appreciable differences between MODIS retrievals onboard Terra and Aqua, which well exceed aerosol daily variabilities. The reasons may be related with sensor calibration uncertainties, and different algorithms and cloud screening schemes. The big jump between POLDER1 and POLDER2 are associated with the different retrieval algorithms. It appears that POLDER2 data are more consistent with other datasets. The POLDER retrieved Ångström exponent over the land is significant higher than others for the reason of that over the land the retrieval technique is only sensitive to small sized aerosols. Due to its limited spectral sampling and the problems with calibration and cloud screening, the AVHRR products are less informative than other more advanced datasets. MODIS and MISR data reasonably agree with AERONET measurements.

Similarities exist between different datasets as well. The average aerosol load is systematically higher in the Northern Hemisphere, and the highest AOD values occur during the summer season and the lowest during the winter. On regional scale, all aerosol products, MODIS and MISR in particular, have captured the main aerosol features at the right time, i.e., dust outbreak in Sahara and Persian regions, smoke in South America and South Africa, mixtures of smoke and dust in Sahel, and pollution downstream of North America, East Asia, and Europe.

This extensive inter-comparison study shows GCM aerosol optical depths are biased a little low, and the Ångström exponent values are much smaller than satellite and ground measurements. The validation study points to the need to increase them. Since in our model the aerosol effective radii are rather arbitrarily specified to convert mass loadings from transport model simulations into optical depths, by reducing the aerosol effective radii specified in the GCM from the near 1.0 micron average value to about 0.2 or 0.3 μm, as suggested by the observed Ångström exponent and Figure 5, we could not only increase our A values but also make the AOD climatology more consistent with the observations (for the same amount of aerosols, smaller particles are more effective in scattering and absorbing light.). This is reinforced by the recent analysis of AERONET spectral optical depths showing that aerosol effective radius is more typically of order 0.3 μm (Sato, 2003, private communication) instead of the nearly 1.0 μm average value in the SI2000 model. However reducing particle sizes alone cannot improve the

agreement of seasonality between the model and the measurements. How to get the global aerosol seasonality right and further improve the model performances on regional scale are our ongoing research topics. It is expected by bringing up GCM clear sky aerosol optical depth to match that of satellite data would increase aerosol radiative forcing ΔF_R by about 30% following the relationship:

$$\Delta F_R = -\frac{S_0}{4} T_{atm}^2 (1-N)(1-a)^2 2\beta\tau$$

where T_{atm} is the transmittance of the atmosphere above the aerosol layer, N is the fraction of sky covered by clouds, a is the albedo of underlying surface, b is the fraction of radiation scattered by aerosol into the upper hemisphere and τ is the aerosol layer scattering optical depth (Charlson et al. 1992).

References

Abdou, WA, DJ Diner, JV Martonchik, CJ Bruegge, RA Kahn, BJ Gaitley, and KA Crean. 2005. "Comparison of coincident MISR and MODIS aerosol optical depths over land and ocean scenes containing AERONET sites." *Journal of Geophysical Research* in press.

Charlson, RJ, SE Schwartz, JM Hales, RD Cess, JA Coakley, Jr., JE Hansen, and DJ Hoffmann. 1992. "Climate forcing by anthropogenic aerosols." *Science* 255, 423-430.

Chin, M, P Ginoux, S Kinne, O Torres, BN Holben, BN Duncan, RV Martin, JA Logan, A Higurashi, and T Nakajima. 2002. "Tropospheric aerosol optical thickness from the GOCART model and comparisons with satellite and sun photometer measurements." *Journal of Atmospheric Science* 59, 461-483.

Fuller, KA, WC Malm, and SM Kreidenweis. 1999. "Effects of mixing on extinction by carbonaceous particles." *Journal of Geophysical Research* 104, 15,941-15,954.

Hansen, JE, and LD Travis. 1974. "Light scattering in planetary atmospheres." *Space Science Review* 16, 527-610.

Hansen, J, W Rossow, B Carlson, A Lacis, L Travis, A DelGenio, I Fung, B Cairns, M Mishchenko, and M Sato. 1995. "Low-cost long-term monitoring of global climate forcings and feedbacks." *Climatic Changes*, 31, 247-271.

Hansen, J, M Sato, and R Ruedy. 1997a. "Radiative forcings and climate response." *Journal of Geophysical Research* 102, 6831-6864.

Hansen, J, M Sato, R Ruedy, A Lacis, K Asamoah, K Beckford, S Borenstein, E Brown, B Cairns, B Carlson, B Curran, S deCastro, L Druyan, P Etwarrow, T Ferede, M Fox, D Gaffen, J Glascoe, H Gordon, S Hollandsworth, X Jiang, C Johnson, N Lawrence, J Lean, J Lerner, K Lo, J Logan, A Luckett, MP McCormick, R McPeters, R Miller, P Minnis, I Ramberran, G Russell, P Russell, P Stone, I Tegen, S Thomas, L Thomason, A Thompson, J Wilder, R Willson, J Zawodny. 1997b. "Forcings and chaos in interannual to decadal climate change." *Journal of Geophysical Research* 102(D22), 25,679-25,720.

Hansen, J, M Sato, R Ruedy, A Lacis, and V Oinas. 2000. "Global warming in the twenty-first century: an alternative scenario." *Proceedings of the National Academy of Sciences of the United States of America*, 97, 9875-9880.

Hansen, M Sato, R Ruedy, J, Lacis, AA, and MI Mishchenko. 1994. "Climate forcing, climate sensitivity, and climate response: a radiative modeling perspective on atmospheric aerosols, Aerosol forcing of climate." RJ Charlson and J Heintzenberg, Eds., John Wiley and Sons, 416pp.

Liu, L, MI Mishchenko, I Geogdzhayev, A Smirnov, SM Sakerin, DM Kabanov, and OA Ershov. 2004. "Global validation of two-channel AVHRR aerosol optical thickness retrievals over the oceans." *Journal of Quantitive Spectroscopy and Radiative Transfer* 88, 97-109.

Penner, JE, SY Zhang, M Chin, CC Chuang, J Feichter, Y Feng, IV Geogdzhayev, P Ginoux, M Herzog, A Higurashi, D Koch, C Land, U Lohmann, M Mishchenko, T Nakajima, G Pitari, B Soden, I Tegen, and L Stowe. 2002. "A comparison of model- and satellite-derived aerosol optical depth and reflectivity." *Journal of Atmospheric Science* 59, 441-460.